Jurnal Penelitian Fisika dan Aplikasinya (JPFA)
Volume 15, Issue 2, 15-25 2025
https://journal.unesa.ac.id/index.php/jpfa/
p-ISSN: 2087-9946
e-ISSN: 2477-1775

Development of Hydroxyapatite-Based Bone Phantoms from Blood Cockle Shells: Effect of Material Composition on X-ray Attenuation

Chika Pricilla Putri Irawan [1,a,*], Devina Rayzy Perwitasari Sutaji Putri [1,b], Rahmawati Munir [1,c], and Zetsaona Sihotang[1,d]

[1] Department of Physics, Faculty of Mathematics and Natural Sciences, Mulawarman University

e-mail: [a] pricillachika8@gmail.com, [b] devina_rayzy@fmipa.unmul.ac.id
* Corresponding Author

Received: 12 August 2025; Revised: 24 October 2025; Accepted: 30 December 2025

Abstract

Radiological phantom is a teaching and simulation tool designed to replicate the physical properties and characteristics of human body tissues, primarily for the evaluation of medical imaging. One alternative material for phantom fabrication is the blood cockle shell (Anadara granosa), which contains hydroxyapatite (HA). This study aims to investigate the effect of varying material compositions on the linear attenuation coefficient (μ) of X-rays in bone phantoms, as well as to determine the optimal composition that approximates the reference values of human bone. The research method involved mixing rice bran, resin, and HA powder synthesized from blood cockle shells in varying HA compositions of 20g, 25g, 40g, and 50g. Each phantom was then scanned using a CT scanner to obtain CT Number values, which represent the linear attenuation coefficient (μ) values. The results showed that the correlation between composition and μ value was not entirely linear, due to the uneven distribution of HA and the presence of voids within the phantom structure. Among the four samples, the phantom with 40 grams of HA (Phantom 3) demonstrated the closest approximation to cortical bone characteristics, with an average CT Number of 1102.15 HU and a μ value of 0.441 cm^{-1}, approximating the attenuation coefficient of human cortical bone. These findings highlight the potential use of waste materials such as blood cockle shells as a main material for bone phantoms that can closely mimic human bone properties.

Keywords: *attenuation coefficient, hydroxyapatite, phantom.*

How to cite: Irawan CPP, Putri DRPS, Munir R, and Sihotang Z. Development of Hydroxyapatite-Based Bone Phantoms from Blood Cockle Shells: Effect of Material Composition on X-ray Attenuation. *Jurnal Penelitian Fisika dan Aplikasinya (JPFA)*, 15(1): 1-8. DOI: https://10.26740/jpfa.v15n2.p15-25

INTRODUCTION

Phantoms are didactic tools in medical imaging employed to simulate human body tissues, meticulously designed to replicate the composition and structure as closely as possible to human anatomy. Beyond their role as teaching aids in medical imaging education, phantoms also serve as crucial test instruments for assessing the suitability and performance of radiological equipment [1]. For radiological investigations and evaluations, phantoms must produce imaging data that are comparable to those of human subjects in order to be used for calculating radiation dose and the transmission of absorption of radiation within the human body. Likewise, phantom materials for X-ray imaging applications must be thoroughly described in terms of how they interact with X-ray

photons, especially in terms of inelastic scattering and X-ray absorption. The materials utilized in phantoms must, at least within the specified range of photon energy, closely mimic the interaction qualities of the tissues or materials they are replacing [2].

Previous studies have utilized various materials for bone phantom fabrication, including chicken bone waste [3] and clam shells [4]. These investigations primarily focused on assessing phantom quality based on the influence of material composition. However, there remains a gap in research specifically exploring the potential of hydroxyapatite (HA) content within blood cockle shells as a foundational material for radiology bone phantoms. Research [4] indicates that the calcium present in cockle shells primarily as calcium carbonate ($CaCO_3$) [5], that can be decomposed into calcium oxide (CaO) and hydroxyapatite ($Ca_{10}(PO_4)_6(OH)_2$). Hydroxyapatite is particularly relevant due to its crystal structure, which closely resembles that of natural bone. As a hexagonal calcium phosphate compound, hydroxyapatite is considered a promising member of the calcium phosphate family for tissue engineering applications. The synthesis of hydroxyapatite can be widely achieved by leveraging natural calcium sources through various methods, such as sol-gel, wet precipitation, and calcination [6].

In other research [7], phantoms synthesized from silicone rubber were tested to determine their linear attenuation coefficient (μ) values that approximate human soft tissue, based on the phantom's CT Number (Hounsfield Unit/HU) [8]. Medical physics applications need the determination of a material's attenuation coefficient (μ), which represents the material's qualities and appropriateness for radiation investigations [9]. The linear attenuation coefficient (μ) can also be defined as a material's ability to absorb incoming radiation. When radiation passes through a material, the intensity of the radiation entering it will be different from the intensity exiting it. This is a result of the material's attenuating properties [10]. The reduction in radiation intensity is caused by the absorption and scattering of primary photons from the X-ray tube [11–13]. In a subsequent study [14] measured the CT Number (HU) of phantoms made from eggshells, with varying the CT-Scan voltage settings. The CT Number represents a material's ability to attenuate X-rays, which is directly related to its elemental composition [8,15]. The HU scale is defined as a quantitive scale used to provide information regarding the radiodensity of a tissue. This scale also offers accurate density information for the specific tissue type being examined. The HU scale is capable of expressing μ with higher precision given its contrast scale of 0.1% per CT Number [7].

Currently, a significant challenge is the high cost and limited availability of phantoms for medical imaging education and practical training. This research aims to address this by developing a bone phantom utilizing blood cockle shells as the primary material. The synthesis process of blood cockle shells through controlled calcination to yield hydroxyapatite (HA) is a distinct novelty of this study. The calcination method is employed to eliminate organic compounds and water, thereby obtaining purified hydroxyapatite and potentially increasing its yield. A key advantage of using calcination is its ability to thermally decompose organic components in the bone and eradicate any genetics markers of disease, thus ensuring a high level of biological safety [6]. Through CT-Scan imaging techniques, this study focuses in evaluating the radiological characteristics of the resulting phantom, particularly its CT Number and μ values. These values will be meticulously compared against human cortical bone references to ascertain the phantom's degree of suitability and effectiveness in simulating authentic bone tissue. Ultimately, this investigation seeks to demonstrate that the developed phantom can serve as an affordable, effective, and representative alternative radiological model for both study purposes and the evaluation of medical imaging

systems [16].

METHOD

Bone phantom fabrication involved several key processes. First, raw blood clam shells were meticulously cleaned to remove any remaining tissue and impurities. They were then dried in an oven at 90°C for 15 mins to eliminate residual organic material from their surfaces. Subsequently, the clam shells underwent calcination in a furnace at 1000°C for 6 h. This step was crucial for converting their calcium content to CaO and facilitating their pulverization. The calcined shells were then finely blended and sieved using a 140 mesh to eliminate non-uniform particles. Following this, the CaO powder was combined with 600 ml of deionized water and 54 g of ammonium dihydrogen phosphate in a hydrothermal process. This reaction was carried out using a magnetic stirrer at 300 rpm, a temperature of 90°C, for 6 hours [17]. This hydrothermal process served as the synthesis step to obtain HA. The resulting solution was then oven-dried at 120°C for 12 hours and subsequently calcined again in a furnace at 900°C for 1 hour [18]. Then purified HA powder mixed with 20 gr of rice bran, 100 ml of resin, and 0,5 gr of catalyst. The HA compositions was varied across four samples, specifically 20 gr, 25 gr, 40 gr, and 50 gr. The entire mixture was stirred until homogeneous and poured into plastic molds with fixed dimensions of 10.5 cm in length, 8 cm in width, and 4 cm in height. The molds were then gently tapped or vibrated to minimize trapped air bubbles within the mixture, allowing it to rise to the surface and escape. Finally, the phantoms were dried in an oven at 90°C for 45 minutes.

Phantom testing was conducted at the Radiology Installation of RSUD A. W. Sjahranie Samarinda, utilizing a GE brand CT-Scan machine. Standard parameters applied for patient examinations at the RSUD A. W. Sjahranie Radiology Installation were used: a tube voltage of 120 kV, tube current of 10 mA, and a slice thickness of 5 mm. The phantom was positioned on the CT-Scan patient table. The resulting phantom images were then processed using ImageJ software to define a Region of Interest (RoI), from which the CT Number (HU) values were obtained. The RoIs were positioned carefully to eliminate any visible air spaces of porosities within the phantom structure by manually locating homogenous areas that accurately depict the hydroxyapatite and resin composite matrix. This method was chosen because adding macro-voids, which are not indicative of the intended bone-mimicking substance, would artificially lower the mean CT Number and increase the standard deviation, leading to a biased estimation of the phantom's effective attenuation. A uniform RoI size of 17 mm^2 was applied on a selected image slice across all phantom samples to ensure consistency and sampling stability [19]. For a more detailed comparison, this study also calculated the CT Number from an image of a human femur bone. An RoI with uniform size was likewise determined on the human femur image to compute its CT Number [20,21]. The human femur pictures were taken as deidentified secondary data from the hospital's old medical records. Prior to the study, all personally identifying information was eliminated in order to protect patient privacy and comply with ethical guidelines.

The CT Number value is representative of the phantom's μ value [7]. Subsequently, the μ values were compared with CT Number values, and an analysis was performed to determine which values most closely approximated the μ and CT Number of human bone. The data acquired included CT Number values from the phantom images obtained via CT-Scan, and μ values calculated using equations:

$$CT\ Number\ (HU) = \frac{\mu_j - \mu_a}{\mu_a} \times k \quad (1)$$

$$\mu_j = \left[\frac{CT\ Number\ (HU) \times \mu_a}{k}\right] + \mu_a \quad (2)$$

where μ_j is the tissue attenuation coefficient, μ_a is water attenuation coefficient ($\mu_a = 0.21$ cm^{-1}), and k is a constant factor with a value of 1000 [6,7,22].

Furthermore, the attenuation coefficient (μ) value obtained from these tests will be used to calculate the Half Value Layer (HVL) with the following equation:

$$HVL = \frac{\ln(2)}{\mu} \quad (3)$$

where μ is the tissue attenuation coefficient (cm^{-1}) [23–26].

To determine the concentration of calcium compounds in this study, one gram of the phantom sample was characterized using Atomic Absorption Spectroscopy (AAS). The purpose of this test was to measure the amount of CaO, which serves as a primary indicator of the precence of synthesized HA within the resin-based matrix.

RESULTS AND DISCUSSION

The resulting phantom images can show the density of each phantom. A tissue's density is a key factor on determining its ability to attenuate X-rays before they reach the detector. This directly influences how the tissue is displayed in the final image. Denser tissues attenuate more X-rays, appearing brighter in the image and yielding a positive CT Number. Conversely, less dense tissues attenuate fewer X-rays, resulting in more transmitted radiation, a darker image, and a negative CT Number [8]. Overall, it can be observed in Figure 1 that phantom 1 is dominated by dark gray tones with numerous black spots, representing air voids caused by low structural density. Additionally, a few conspicuous white spots are visible, representing HA powder clumps; these areas exhibit high density due to their bone-mimicking properties [6,27]. This indicates an uneven or non-homogeneous distribution of materials within the phantom. In phantom 2, the gray tones appear more uniform with fewer black and white spots compared to Phantom 1, indicating a better material distribution and structural density. Furthermore, phantom 3 is dominated by light gray to white tones, reflecting a higher density variation compared to phantoms 1 and 2. Notably, this image does not show significant dark or bright spots, suggesting a more compact structure with relatively homogeneous material distribution. In contrast, phantom 4 displays a dark central area surrounded by numerous black spots. There are also extensive dark gray regions, which signify lower density and a non-homogeneous structural distribution.

The CT images in Figure 1 were then processed using ImageJ software to get the CT Number value by placing the RoI in areas free from air voids within each phantom. The resulting CT Number values, which consist of a mean and standard deviation (SD) for the phantoms, are represented in Table 1. These values are directly proportional to the structural density of the phantom [28].

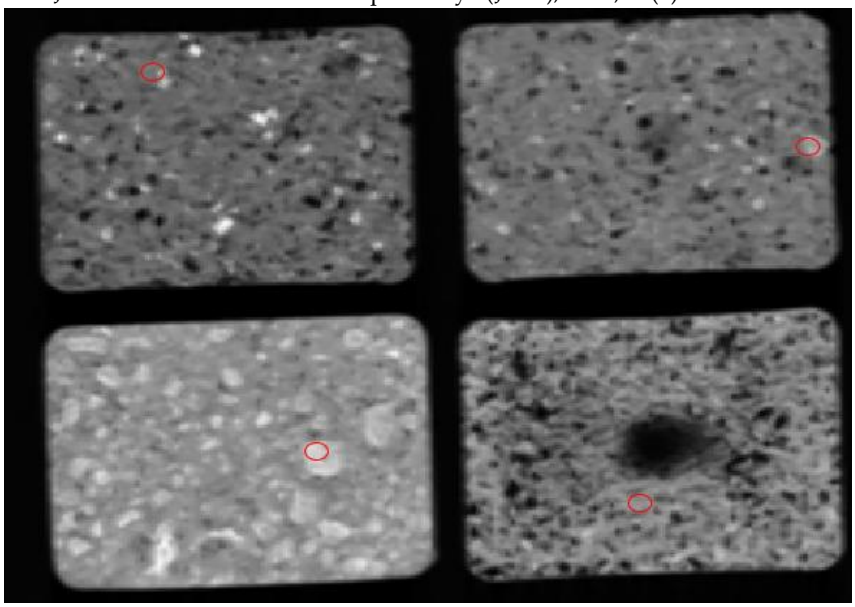

Figure 1. Images of the phantom with RoI. Phantom 1 (top left), Phantom 2 (top right), Phantom 3 (bottom left), and Phantom 4 (bottom right).

Table 1 shows significant differences in the CT Number values among the phantoms. Phantom 1 has a mean CT Number that is close to the range for trabecular (spongy) bone (148 to 661 HU) [29], although its high SD indicates significant density variation within the defined RoI. Phantom 2 shows an increase in mean density, with its value still falling within the trabecular bone CT Number range. Phantom 3 has a mean CT Number value that is consistent with cortical bone characteristics (CT Number range of 586 to 1988 HU) [29,30] and its more homogeneous distribution evident from both the image and its low SD value. Conversely, phantom 4 shows decrease in mean density, suggesting a non-uniform HA distribution despite having the highest HA composition. The mean CT Number values for the phantoms and the human femur bone were then used to calculate the μ value using Equation 2.

Tabel 1. CT Number values.

Sample	HA Composition (gr)	CT Number (HU) Mean ± SD
Phantom 1	20	253.43 ± 149.17
Phantom 2	25	502.19 ± 196.93
Phantom 3	40	1102.15 ± 112.98
Phantom 4	50	451.89 ± 87.00
Femur bone	-	1374.07 ± 182.26

The calculation results show a direct correlation between the μ value and the mean CT Number within the phantom's RoI. The larger the mean CT Number, the greater the μ value and vice versa. This proves that the CT Number can serve as an indicator representing a material's X-ray attenuation capability. Of the four phantom samples, the μ value of phantom 3 is the closest to that of a human femur bone. This suggests that the attenuation capability of phantom 3's RoI

approximates that of human bone, which is a type of cortical bone, as evidenced by the resulting image and the phantom's mean CT Number and μ values. Furthermore, the chemical characterization via AAS showed a CaO content of 12.54% within the 1 g of phantom 3 sample. This quantitive result demonstrates that the blood cockle shells were successfully converted into calcium-rich substance by the calcination hydrothermal procedures.

Table 2. Linear attenuation coefficient (μ) value and HVL value.

Sample	HA Composition (gr)	μ (cm^{-1})	HVL (cm)
Phantom 1	20	0.263	2.633
Phantom 2	25	0.315	2.197
Phantom 3	40	0.441	1.570
Phantom 4	50	0.305	2.273
Femur bone	-	0.498	1.390

The variations in CT Number and μ values among the four phantom samples were not linear with the addition of HA composition, which is due to the phantom's low homogeneity as evidenced by density variations in the resulting images. The non-homogeneity of the phantom structure was caused by the material mixing method. Resin-containing mixtures have the potential to form clumps and create air bubbles, especially if the mixing process is too fast, a problem that can be minimized by slow and careful stirring [31]. Consequently, the improper mixing method used during phantom fabrication led to the formation of air voids and an uneven distribution of HA powder during the drying process. This condition contributed to the CT Number values varying both within and between samples, which is why the mean CT Number and μ values were not entirely linear with the increase in HA.

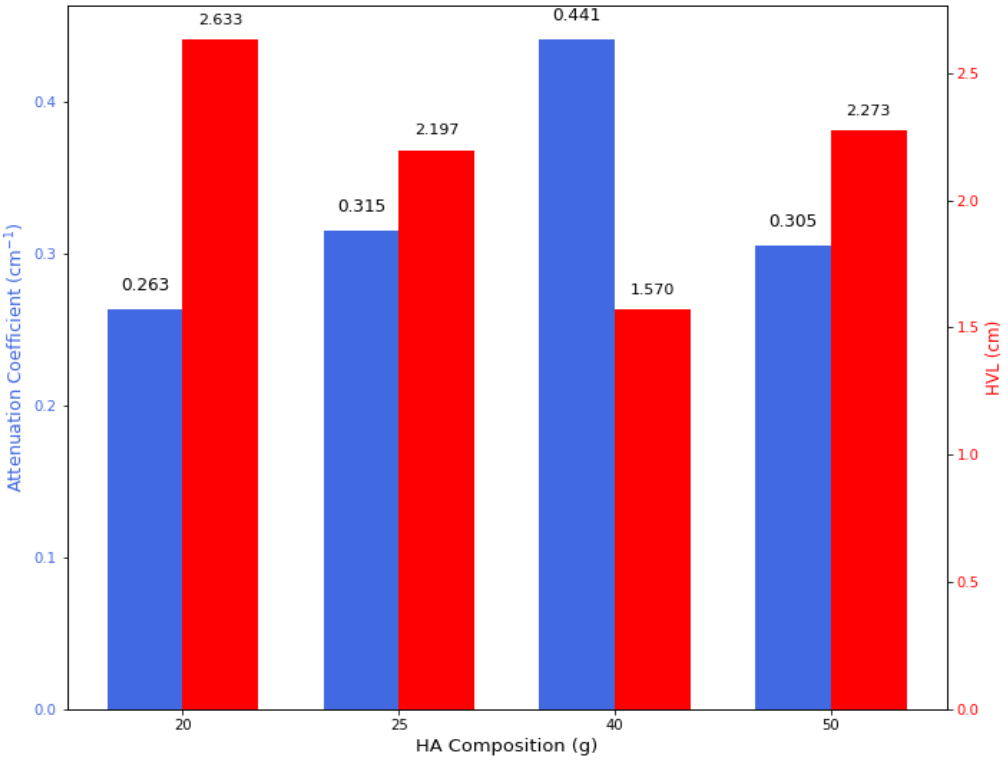

Figure 2. Phantom's linear attenuation coefficient (μ) and HVL.

Figure 2 shows a bar graph of the μ and HVL values for the four phantom samples. The pattern demonstrates that the addition of HA increased the μ value up to a composition of 40 grams, after which is decreased at the 50 gram HA composition. Those μ value is inversely proportional to the resulting HVL value, in accordance with Equation 3 [26]. Consequently, the HVL value shows a decreasing trend as the HA composition increases, up to the 40 gram point. Conversely, the HVL value experiences an increase at the 50 gram HA composition, reflecting the decrease in μ value. The HVL value itself represents the thickness of a material required to reduce the intensity of an X-ray beam passing through it to half of its initial dose value [32]

Nevertheless, the phantom samples in this study, as a whole, still show potential for use as bone phantoms in the field of radiology. This is because of the HA content, which was synthesized from blood cockle shells. The phantom images show that the clumps of HA powder produced white images resembling bone, resulting in high maximum CT Number values. The potential of phantoms containing HA would be maximized with a structure that has a high degree of homogeneity and a more even distribution of HA. A more stable image density would produce attenuation properties closer to human bone, which would be useful for Quality Assurance (QA) applications in evaluating the uniformity of CT-Scan images.

CONCLUSION

The creation of low-cost bone phantom using HA made from blood cockle shells was effectively demonstrated in this study. The results offer important insights into waste-to-material transformation for medical physics, even if the link between HA composition and the μ value was not totally linear because of material non-homogeneity and air gaps. Phantom 3 (40 g HA) emerged as the optimal sample, yielded a mean CT Number of 1102.15 HU, which falls within the CT Number range for cortical bone (586 HU to 1988 HU). This is also consistent with the μ value of 0.441 cm^{-1} for Phantom 3, which was calculated from the mean CT Number and approximates the μ value of a human femur, a type of cortical bone. A CaO concentration of 12.54% on phantom 3 sample was verified by AAS, confirming that the calcination procedure was succesfull in producing the high-purity mineral components needed for bone simulation. This alignment demonstrates that biological waste can be designed into a radiological instrument that is functionally representative. Ultimately, this research offers a sustainable and affordable alternative for medical imaging education and quality assurance, provided that future fabrications implement improved mixing techniques to enhance structural homogeneity.

AUTHOR CONTRIBUTIONS

Chika Pricilla Putri Irawan: Conceptualization, Methodology, Investigations, Data Curation, Analysis, and Writing-Orginal Draft. Rahmawati Munir: Conceptualization, Methodology, Validation, Supervision, and Writing – Review & Editing. Devina Rayzy Perwitasari Sutaji Putri: Resources, Conceptualization, Methodology, Validation, Supervision, and Writing – Review & Editing. Zetsaona Sihotang: Validation, Formal Analysis, Supervision, and Writing – Review & Editing.

DECLARATION OF COMPETING INTEREST

The authors declare that the work reported in this manuscript is not influenced by any financial conflicts of interest or personal relationships.

DECLARATION OF ETHICS

The authors declare that the research was conducted in accordance with established scientific and ethical principles, and the manuscript is an original work, free of plagiarism.

DECLARATION OF ASSISTIVE TECHNOLOGIES IN THE WRITING PROCCESS

The authors affirm that Generative Artificial Intelligence and other assistive technologies were not excessively utilized in the research and writing processes of this manuscript.

REFERENCES

[1] Mufida W, Utami AP and Dewi SN. Pembuatan Phantom Radiologi Berbahan Dasar Kayu Lokal Sebagai Pengganti Tulang Manusia. *Jurnal Imejing Diagnostik (JImeD)*. 2020; **6**(1): 7–10. DOI:https://10.31983/jimed.v6i1.5404.

[2] Ma X, et al. X-Ray Attenuation of Bone, Soft and Adipose Tissue in CT from 70 to 140 KV and Comparison with 3D Printable Additive Manufacturing Materials. *Scientific Reports*. 2022; **12**(1): 1–13. DOI:https://10.1038/s41598-022-18741-4.

[3] Sari AW, Olivia Hidayati A, Mahdo Hapiza D and Ridwan A. Pembuatan Phantom Radiologi Menggunakan Cangkang Kerang Sebagai Pengganti Bahan Tulang. *Journal Online of Physics*. 2023; **8**(2): 50–55. DOI:https://10.22437/jop.v8i2.22303.

[4] Noorma K, et al. IDENTIFIKASI POTENSI CANGKANG KERANG DARAH LOKAL DESA KUTAI LAMA DAN PEMANFATAANNYA UNTUK PENURUNAN KADAR LOGAM BESI (Fe2+). *Prosiding 4th Seminar Nasional Penelitian & Pengabdian Kepada Masyarakat*. 2020; : 17–22.

[5] Nuringtyas KD. UJI KEKERASAN CANGKANG KERANG DARAH (Anadara Granosa) SEBAGAI BAHAN ABRASIF UNTUK PEMOLESAN BASIS GIGI TIRUAN LEPASAN AKRILIK HEAT CURED. 2018; : 0–22. Available from: http://www.uib.no/sites/w3.uib.no/files/attachments/1._ahmed-affective_economies_0.pdf%0Ahttp://www.laviedesidees.fr/Vers-une-anthropologie-critique.html%0Ahttp://www.cairn.info.lama.univ-amu.fr/resume.php?ID_ARTICLE=CEA_202_0563%5Cnhttp://www.cairn.info.

[6] Afifah F and Cahyaningrum E. SINTESIS DAN KARAKTERISASI HIDROKSIAPATIT DARI TULANG SAPI (Bos Abstract . Cow Bone Has a High Hydroxyapatite Composition , so It Can Be Determined as a Preliminary Material in the Synthesis of Hydroxyapatite . Cow Bone Has an Inorganic Composition Consi. 2020; **9**(3): 189–196.

[7] Ansar A, Nurhasmi N and Amir A. Pengukuran Koefisien Atenuasi Fantom Berbasis Silicone Rubber RTV 48. *Wahana Fisika*. 2022; **7**(1): 43–53. DOI:https://10.17509/wafi.v7i1.41219.

[8] Gupta K, et al. CLINICAL APPLICATIONS AND TECHNICAL IMAGES OF HOUNSFIELD UNITS IN CLINICAL APPLICATIONS AND TECHNICAL IMAGES OF. 2024; (July). DOI:https://10.1729/Journal.40796.

[9] Zuber SH, et al. Attenuation Coefficients of Soy-Lignin Bonded Rhizophora Spp. Particleboard as a Potential Phantom Material Using Monte Carlo GATE Siti. *BioResources*. 2024; **19**(4): 8920–8934.

[10] Diartama AAA, Sari PAPR, Prasetya IML and Eka IP. Effect of Variations in Material Concentrations on The X-Ray Attenuation Coefficient Value: Study on Chicken Bone-

Radiologic Phantom. *International Journal of Allied Medical Sciences and Clinical Research (IJAMSCR)*. 2022; **10**(1): 125–129.

[11] Boiset GR, et al. X-Ray Spectrometry Applied for Determination of Linear Attenuation Coefficient of Polymer-Based Samples as Radiologically Tissue-Equivalent Materials. *Brazilian Journal of Radiation Sciences*. 2023; **11**(1A): 01–14. DOI:https://10.15392/2319-0612.2023.2166.

[12] Umar M, Saidu A, Aliyu J and Shehu A. Investigation of Attenuation Properties of Liquid Materials by Gamma Absorption-Scattering Method. *International Journal of Research and Innovation in Applied Science*. 2022; **07**(10): 76–81. DOI:https://10.51584/ijrias.2022.71006.

[13] Mohammed SI and Taqi AH. Mass Attenuation Coefficient of Electromagnetic Radiation for Human Tissues. *Journal of Radiation Research and Applied Sciences*. 2025; **18**(1): 101255. DOI:https://10.1016/j.jrras.2024.101255.

[14] Yusmaliani E, Astuty SD and Dewang S. JFT : Jurnal Fisika Dan Terapannya Pembuatan Dan Uji Nilai HU Jaringan Tulang Buatan Berbahan Dasar. 2025; **12**: 102–116. DOI:https://10.24252/jft.v12i1.58374.

[15] Jeong DK, et al. Effects of Energy Level, Reconstruction Kernel, and Tube Rotation Time on Hounsfield Units of Hydroxyapatite in Virtual Monochromatic Images Obtained with Dual-Energy CT. *Imaging Science in Dentistry*. 2019; **49**(4): 273–279. DOI:https://10.5624/isd.2019.49.4.273.

[16] Tuğrul T and Eroğul O. Analysis of Water-Equivalent Materials Used during Irradiation in the Clinic with XCOM and BEAMnrc. *Journal of Radiation Research and Applied Sciences*. 2019; **12**(1): 455–459. DOI:https://10.1080/16878507.2019.1708576.

[17] Sari RN, Fransiska D, Dewi FR and Sinurat E. Karakteristik Sediaan Hidroksiapatit Dari Cangkang Kerang Simping (Amusium Pleuronectes) Dengan Perlakuan Suhu Dan Waktu Sintesis. *Jurnal Pascapanen dan Bioteknologi Kelautan dan Perikanan*. 2022; **17**(1): 31. DOI:https://10.15578/jpbkp.v17i1.797.

[18] Ervina, Fadli A and Amri I. APLIKASI SHRINKING CORE MODEL PADA SINTESIS HIDROKSIAPATIT DARI KULIT KERANG DARAH (Anadara Granosa) DENGAN MENGGGUNAKAN METODE HIDROTERMAL SUHU RENDAH. 2016; : 1–6.

[19] Marwah SA, Saharani N, Astuty SD and Dewang S. DESAIN FANTOM BERBASIS GELATIN DAN Zn UNTUK. 2024; **27**(2).

[20] Chattopadhyay S. An Approach to Identify Regions of Interest in Chest X-Ray Images of COVID-19 Patients and Its Clinical Validation: An Indian Study. *Artificial Intelligence Evolution*. 2022; **3**(1): 41–53. DOI:https://10.37256/aie.3120221331.

[21] Widiatmoko ME and Ramadanti S. Nilai Hounsfield Unit (HU) CT-Scan Pada Lesi Paru-Paru Pasien Suspek COVID-19. *Jurnal Kesehatan Vokasional*. 2023; **8**(3): 174. DOI:https://10.22146/jkesvo.78738.

[22] Jung H. Basic Physical Principles and Clinical Applications of Computed Tomography. *Progress in Medical Physics*. 2021; **32**(1): 1–17. DOI:https://10.14316/pmp.2021.32.1.1.

[23] Khaidir LM, Yusof MFM, Shawkataly AK and Mohamed NS. Determination of Mass Attenuation Coefficient of Jute Reinforced Epoxy Resin Composite as Tissue Equivalent Phantom. *Journal of Physics: Conference Series*. 2024; **2907**(1). DOI:https://10.1088/1742-6596/2907/1/012013.

[24] Ansar A, et al. Analysis of the Attenuation Coefficient of Composite Silicone Rubber and

Gliceryn for Soft Tissue Phantom Applications. *Iranian Journal of Medical Physics*. 2020; **17**(1): 8–13. DOI:https://10.22038/ijmp.2019.38410.1494.

[25] Solihah M, et al. Analisis Pemanfaatan Pasir Besi Dan Batu Apung Sebagai Agregat Beton Perisai Radiasi Sinar-X. *ORBITA: Jurnal Pendidikan dan Ilmu Fisika*. 2023; **9**(1): 167. DOI:https://10.31764/orbita.v9i1.14731.

[26] Rahmawati I, Jumpeno BYEB, Mellawati J and Ramlan R. ANALISIS TINGKAT ABSORPSI BERKAS SINAR-X PADA SINTESIS KOMPOSIT KAKTUS (Opuntia Spp.) DAN TIMBAL (II) ASETAT (Pb(CH3COO)2) SEBAGAI MATERIAL APRON. *GANENDRA Majalah IPTEK Nuklir*. 2024; **26**(2): 82. DOI:https://10.55981/gnd.2023.6870.

[27] Akbar AF, 'Aini FQ, Nugroho B and Cahyaningrum SE. SINTESIS DAN KARAKTERISASI HIDROKSIAPATIT TULANG IKAN BAUNG (Hemibagrus Nemurus Sp.) SEBAGAI KANDIDAT IMPLAN TULANG. *Jurnal Kimia Riset*. 2021; **6**(2): 93. DOI:https://10.20473/jkr.v6i2.30695.

[28] Februari N, et al. Uji Kesesuaian CT Number Pada Pesawat CT Scan Multislice Di Rumah Sakit Sunset Vet Kuta Akademi Teknik Radiodiagnostik Dan Raditerapi Bali , Indonesia Salah Satu Program QC Yang Digunakan Dalam Penggunaan Pesawat CT-Scan . CT Number Berdasarkan Hasil Obse. 2024; **2**(1).

[29] Saija C, et al. Evaluation of a Three-Dimensional Printed Interventional Simulator for Cardiac Ablation Therapy Training. *Applied Sciences (Switzerland)*. 2024; **14**(18). DOI:https://10.3390/app14188423.

[30] Vikas Chougule, B. B Ahuja and Arati Mulay. Clinical Case Study Spine Modeling for Minimum Invasive Spine Surgeries. *International Conference on Precision, Meso, Micro and Nano Engineering (COPEN)*. 2018; (March): 96–102.

[31] Alamsyah, Hidayat T and Iskandar AN. PENGARUH PERBANDINGAN RESIN DAN KATALIS TERHADAP KEKUATAN TARIK KOMPOSIT FIBERGLASS-POLYESTER UNTUK BAHAN PEMBUATAN KAPAL. *Zona Laut : Jurnal Inovasi Sains Dan Teknologi Kelautan*. 2021; **2**(3): 92–98.

[32] Nouchi S, et al. A Pilot Study of Half-Value Layer Measurements Using a Semiconductor Dosimeter for Intraoral Radiography. *Imaging Science in Dentistry*. 2023; **53**(3): 217–220. DOI:https://10.5624/isd.20230039.